



University
of Glasgow

Jassim Katwan, Osama (2010) *Discrete modelling of heat transfer*.
MSc(R) thesis, University of Glasgow.

<http://theses.gla.ac.uk/1602/>

Copyright and moral rights for this thesis are retained by the author

A copy can be downloaded for personal non-commercial research or
study, without prior permission or charge

This thesis cannot be reproduced or quoted extensively from without first
obtaining permission in writing from the Author

The content must not be changed in any way or sold commercially in any
format or medium without the formal permission of the Author

When referring to this work, full bibliographic details including the
author, title, awarding institution and date of the thesis must be given

Discrete modelling of heat transfer

Osama M. Jassim Katwan

October, 2009

Thesis submitted in fulfilment of the requirement for a Degree of
Master of Science, University of Glasgow

Abstract

The research involves the development of a discrete lattice approach for modelling heat transfer, which can be an attractive alternative to other numerical approaches, such as the finite element method. In this work, the spatial arrangement of the lattice elements is determined by the Delaunay triangulation and the Voronoi tessellation. The objective of the present work is to investigate in more detail this type of lattice model for heat transfer.

In the lattice models studied here the domain to be analysed is discretised by a network of discrete lattice elements. The spatial arrangement of these elements is determined by connecting nodes placed within the domain. There are two methods to determine the connections between the nodes in the domain. In the first one, the connections are defined as the edges of the Delaunay triangulation. In the second method, the nodes are defined by the edges of Voronoi cells, based on a Voronoi tessellation of the domain. These connections define the arrangement of the pipe elements, which are used to perform the heat transfer analysis. The cross-sections of the pipe elements for the two approaches are chosen in several different ways to be consistent with the discretisation approach.

It was shown that with this approach, analytical solutions could be represented accurately. Several stationary and non-stationary heat transfer problems were analysed. The performance of the two approaches was evaluated by comparing the numerical results with analytical solutions. Both temperature and flux distributions were studied.

Contents

1	Introduction	12
1.1	Outline	13
2	The lattice method for heat transfer	15
2.1	Introduction	15
2.2	Governing equation	15
2.3	Discretised governing equation	16
2.3.1	Steady state problems	17
2.3.2	Transient problems	17
2.4	Discussion	20
3	Discretisation approaches	21
3.1	Random point generation	21
3.2	Lattice generation	22
3.3	Cross-sectional area of lattice element	23
3.3.1	Voronoi and Delaunay scaling	25
3.3.2	Average cross-sectional area	25
3.3.3	Centroidal method	26
3.4	Flux calculation	27
3.5	Discussion	29

Contents

4	Results and discussions	31
4.1	Introduction	31
4.2	Steady state analyses of a homogeneous square domain	31
4.2.1	Voronoi scaling	33
4.2.2	Delaunay scaling	37
4.2.3	Centroidal scaling	38
4.2.4	Constant cross-sectional area	40
4.3	Transient analyses	41
4.4	Effect of boundary layer on accuracy	45
4.5	Steady state analyses of homogeneous domain with isolated inclusion	51
4.6	Discussion	52
5	Conclusions and suggestions for future studies	57
5.1	Conclusions	57
5.2	Suggestions for future studies	58
	Appendix	61

Nomenclature

Δt Time increment

ℓ Length of domain

ω_i Eigenvalue of the i th mode of the system

ρ Density

ρ_p Density of points

A_i Area calculated from the Voronoi or Delaunay scaling

C Specific heat capacity

C_1, C_2 Centroid of Delaunay triangle

k Lattice element conductivity

m_d Minimum distance

n Number of lattice elements.

P_1 Number of nodes inside the domain

q Flux

r Inclusion radius

T Temperature

Contents

t Total time of the analysis

List of Figures

2.1	Lattice element.	17
3.1	Point distribution method: (a) Quasi-uniform point distribution, (b) Non-uniform point distribution.	22
3.2	Delaunay domain discretisation for a set of nodes placed in the domain.	24
3.3	Voronoi domain discretisation for a set of nodes placed in the domain.	24
3.4	Voronoi scaling: Definition of the cross-sectional area of a lattice element determined by Delaunay discretisation.	25
3.5	Delaunay scaling: Definition of the cross-sectional area of a lattice element determined by Voronoi discretisation.	26
3.6	A section of Delaunay triangulation showing the cross-sectional area based on the centroidal method.	28
3.7	Flux calculation for a Delaunay element node.	29
4.1	Domain geometry and boundary condition.	32
4.2	Delaunay domain discretisation based on a quasi-uniform point distribution.	33
4.3	Voronoi domain discretisation based on a quasi-uniform point distribution.	34
4.4	Delaunay domain discretisation based on a non-uniform point distribution.	34
4.5	Voronoi domain discretisation based on a non-uniform point distribution.	35

List of Figures

4.6	Comparison of numerical and analytical solution for a quasi-uniform lattice.	36
4.7	Comparison of numerical and analytical solution for a non-uniform lattice.	36
4.8	Comparison of numerical and analytical solution for a quasi-uniform lattice.	37
4.9	Comparison of numerical and analytical solution for a non-uniform lattice.	38
4.10	Comparison of numerical and analytical solution using the centroidal method for a quasi-uniform lattice.	39
4.11	Comparison of numerical and analytical solution using the centroidal method for a non-uniform lattice.	39
4.12	Comparison of numerical and analytical solution using a constant cross-sectional area for a quasi-uniform lattice based on the Delaunay discretisation.	40
4.13	Comparison of numerical and analytical solution using a constant area for a non-uniform lattice based on the Delaunay discretisation.	41
4.14	Comparison of numerical and analytical solution using a constant area for a uniform lattice based on the Delaunay discretisation.	42
4.15	Comparison of numerical and analytical solution using a constant area for a non-uniform lattice based on the Voronoi discretisation.	42
4.16	Temperature distribution along in the x-direction for $y = 0.5$ for time steps varying from 0 to 1 using a (a) quasi-uniform lattice and (b) non-uniform lattice based on the Delaunay discretisation.	44
4.17	Temperature distribution along the x -direction for $y = 0.5$ for the (a) quasi-uniform lattice (b) non-uniform lattice based on the Voronoi discretisation.	46
4.18	Transient analyses of the domain with comparison to the analytical solution: (a) Delaunay discretisation, (b) Voronoi discretisation.	47

List of Figures

4.19	Delaunay and Voronoi domain discretisation based on a non-uniform point distribution.	48
4.20	Comparison of numerical and analytical solution at $y = 0$. The boundary conditions are described only on the left and right of the domain.	49
4.21	Comparison of numerical and analytical solution at $y = 0.3$. The boundary condition are described as a frame with the thickness of 0.1ℓ	50
4.22	Comparison of numerical and analytical solution at $y = 0.3$. The boundary conditions are described as a frame with the thickness of 0.2ℓ	50
4.23	Domain discretisation with an inclusion: (a) The domain discretisation (b) The discretisation of the inclusion.	53
4.24	Temperature distribution along the x-direction for $y = 0.5$: (a) The entire specimen (b) Detail around the inclusion.	54
4.25	Flux around an inclusion obtained by the Delaunay discretisation. The solid and dashed lines represent the numerical and analytical solution, respectively.	55

List of Tables

4.1	Properties of the domain	32
4.2	Properties of the domain	43
4.3	Physical properties of the domain.	48
4.4	Properties of the domain with an inclusion	51

Preface

The work presented in this Master's thesis is the result of a research project on the performance of the lattice method in heat transfer carried out between January 2007 and October 2009 at the Civil Engineering Department, University of Glasgow under the supervision of Dr. Chris Pearce and Dr. Peter Grassl.

I would like to thank my supervisors for their valuable discussions and for their understanding and time. Furthermore, I would like to thank all my colleagues in the department for sharing their knowledge and for giving valuable advice and support with great willingness to help.

Finally, I thank my family for always being there for me and financing my study.

Osama Moufaq Jassim Katwan

1 Introduction

The field of computational mechanics continues to develop rapidly, largely as a result of the unprecedented success of the Finite Element Method (FEM) and the ever increasing availability of computational resources. Scientists and engineers are now able to investigate extremes of size and condition, beyond the range of physical experiments, through the development and use of so-called virtual laboratories. Despite the success of the FEM, there are a number of alternative computational approaches for the analysis of materials and structures that have proved successful in specific situations and warrant further consideration.

The motivation for this work is the study of heterogeneous materials, through the development of appropriate and efficient computational tools, in order to simulate the interaction of mechanical behaviour with other physical phenomena, such as heat transfer. The macroscopic response of heterogeneous materials can be investigated by considering the influence of processes on the fine scales. However, the FEM may not be the best candidate to solve such problems, since it can struggle to deal with displacement discontinuities and material interfaces without a highly adapted mesh or the introduction of an enrichment technique. A promising alternative is the lattice approach and this is the subject of this thesis.

Within the context of the analysis of multiple physical process, this work focuses on an investigation of the suitability of the lattice approach for modelling heat transport. In the past, discrete lattice models have been used for analysing various physical problems.

1 Introduction

For concrete, lattice models have shown to be capable of describing complex fracture patterns [10, 14, 6, 3, 9]. Furthermore, mass transport can be described by a lattice of conduit elements, which can be linked to the structural lattice to couple fracture and transport processes [5, 13]. A special type of lattice model for the mechanical response and mass transport was proposed recently, which provides mesh-independent and accurate descriptions of basic aspects of the continuum response [4, 2]. In this approach, the cross-sections of structural and transport elements are determined from the Voronoi tessellation of random nodes placed in the structural domain. This modelling approach was further developed to describe the interaction of transport along discrete cracks and the surrounding material by introducing an additional lattice of transport elements [15, 11]. An alternative approach with only one lattice for both the intact material and the cracks was developed by P. Grassl [7] for two dimensions and extended to three dimensions by P. Grassl and J. Bolander[8].

In solving a continuum mechanics problem, the FEM utilises a discretisation of the domain into a finite number of continuum elements (e.g. triangles or quadrilaterals in 2D). In contrast, the lattice method utilises a lattice of simple line elements: truss or beam elements for mechanical problems; pipe elements for heat transfer problems. Therefore, the formulation for the lattice method is relatively straightforward but its effectiveness for solving heat transfer problems requires further investigation. The focus of this work is to investigate various discretisation techniques for the lattice method.

1.1 Outline

The thesis is organised as follows. Chapter 2 will introduce the lattice method and present the formulation for solving both steady-state and transient heat transfer problems. Chapter 3 will focus on two discretisation methods that have been investigated in detail. The first is based on a Delaunay triangulation of the domain under consideration

1 Introduction

and the second is based on the associated Voronoi tessellation. In order to accurately reproduce the continuum solution, this discrete approach relies on an accurate geometric scaling of the individual line elements. Different scaling techniques are presented in Chapter 3. Chapter 4 presents numerical results for both steady-state and transient problems and discusses the results obtained with the different discretisation and scaling techniques presented in Chapter 3. Chapter 5 draws conclusions and discusses future research directions.

2 The lattice method for heat transfer

2.1 Introduction

The lattice approach was used to solve steady state and transient heat transfer analyses in the research carried out. In the modelling of a heterogeneous material such as concrete, the assignment of different material properties to each lattice element can be easily achieved. Moreover the lattice approach has already been shown to be a reliable alternative in the modelling of elasticity and fracture mechanics [3]. Various approaches for discretisation of the domain are discussed in the next chapter. Here attention is focused on the discretised system of equations.

2.2 Governing equation

The domain is discretised into a network of lattice elements, each one considered to be a one dimensional pipe that conducts heat. More details on the discretisation is given in the next Chapter. The one dimensional governing partial differential equation for heat transfer is given by

$$\rho C \frac{\partial T}{\partial t} = -\frac{dq}{d\xi} + Q \quad (2.1)$$

where T is the temperature, ρ is the material density, C is the specific heat capacity,

2 The lattice method for heat transfer

t is time, Q is the volumetric heat generation per unit volume per unit time and q is the heat flux in direction ξ .

The formulation is completed by inclusion of Fourier's law, which is a relationship between the gradient of temperature and the heat flux - known as the thermal constitutive equation. The Fourier law is a linear relationship given as:

$$q = -k \frac{dT}{d\xi} \quad (2.2)$$

where k is the material thermal conductivity. Substituting of Fourier's law into Eq 2.1, gives the governing equation in terms of temperature:

$$\rho C \frac{\partial T}{\partial t} = k \frac{d^2 T}{d\xi^2} + Q \quad (2.3)$$

2.3 Discretised governing equation

Consider a single lattice element, see Figure 2.1, defined by nodes i and j . The unknown nodal temperatures are T_i and T_j and the temperature in each lattice element is assumed to vary linearly between these nodal values as:

$$T(\xi) = \frac{1}{2} ((T_j - T_i) \xi + T_i + T_j) \quad (2.4)$$

where ξ is a local coordinate, varying from $\xi = -1$ at node i to $\xi = +1$ at node j .

Applying the standard Galerkin weighted residual approach, the discrete form of Eq 2.5 [12] is:

$$\mathbf{KT} + \mathbf{CT} = \mathbf{f} \quad (2.5)$$

where \mathbf{K} is the lattice element conductivity matrix, \mathbf{C} is the capacitance matrix, \mathbf{f} is the "force" vector and $\mathbf{T} = (T_i \ T_j)^T$ is the vector of nodal temperatures:

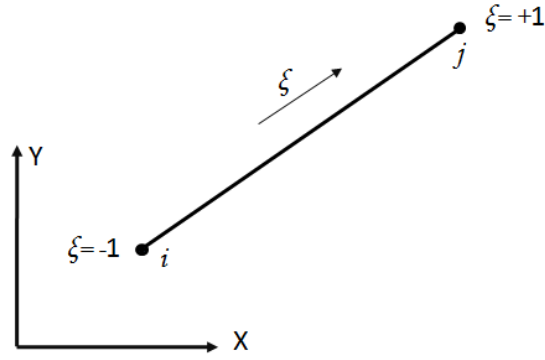


Figure 2.1: Lattice element.

$$\mathbf{K} = \frac{KA}{L} \begin{bmatrix} 1 & -1 \\ -1 & 1 \end{bmatrix}, \quad \mathbf{C} = \frac{\rho CA}{12} \begin{bmatrix} 2 & 1 \\ 1 & 2 \end{bmatrix}, \quad \mathbf{f} = \begin{pmatrix} -q_i A \\ -q_j A \end{pmatrix} \quad (2.6)$$

Here, A is the element cross-sectional area, L is the element length and q_i and q_j are the prescribed nodal fluxes at nodes i and j , respectively. Local heat sources/sinks have been ignored for simplicity, i.e. $Q = 0$.

2.3.1 Steady state problems

The steady state form of Eq 2.5 is derived by removing the time dependence as:

$$\mathbf{KT} = \mathbf{f} \quad (2.7)$$

This system of linear algebraic equations, together with appropriate boundary conditions, can be solved using standard equation solvers.

2.3.2 Transient problems

For a given time interval $\Delta t = t^{n+1} - t^n$ the temperature at time t is defined via a linear interpolation:

2 The lattice method for heat transfer

$$T(t) = \theta T^{n+1} + (1 - \theta) T^n \quad (2.8)$$

where T^n and T^{n+1} are the temperatures at the beginning and end of the time interval and

$$\theta = \frac{1}{\Delta t} (t - t^n) \quad (2.9)$$

which lies in the interval $0 < \theta < 1$.

Therefore the temperature rate is given as:

$$\dot{T} = \frac{1}{\Delta t} (T^{n+1} - T^n) \quad (2.10)$$

Substitution of this approximation into Eq 2.5, yields:

$$\mathbf{K} (\theta \mathbf{T}^{n+1} + (1 - \theta) \mathbf{T}^n) + \frac{1}{\Delta t} \mathbf{C} (\mathbf{T}^{n+1} - \mathbf{T}^n) = \mathbf{f} \quad (2.11)$$

From this finite difference approximation there are a number of possibilities:

1. Forward difference, corresponding to $t = t^n$ and $\theta = 0$:

$$\mathbf{C} \mathbf{T}^{n+1} = (\mathbf{C} - \Delta t \mathbf{K}) \mathbf{T}^n + \Delta t \mathbf{f}^n \quad (2.12)$$

2. Backward difference, corresponding to $t = t^{n+1}$ and $\theta = 1$:

$$(\mathbf{C} + \Delta t \mathbf{K}) \mathbf{T}^{n+1} = \mathbf{C} \mathbf{T}^n + \Delta t \mathbf{f}^n \quad (2.13)$$

3. Central difference, corresponding to $t = t^n + \frac{1}{2} \Delta t$ and $\theta = 0.5$:

$$\mathbf{C} \mathbf{T}^{n+1} = \mathbf{C} \mathbf{T}^{n-1} - 2\Delta t \mathbf{K} \mathbf{T}^n + 2\Delta t \mathbf{f}^n \quad (2.14)$$

2 The lattice method for heat transfer

4. In general, Eq 2.11 is rearranged as follows to give the θ – Method:

$$(\mathbf{C} + \theta\Delta t\mathbf{K}) \mathbf{T}^{n+1} = (\mathbf{C} - (1 - \theta)\Delta t\mathbf{K}) \mathbf{T}^n + \Delta t\mathbf{f}^n \quad (2.15)$$

To solve transient analyses using any of these methods, appropriate initial conditions must be defined at time $t = 0$. In addition, solution stability must be considered. Considering the generic θ – Method, the following conditions must be satisfied to ensure stability [12]:

$$|\lambda| < 1$$

where, $\lambda = (1 - (1 - \theta)\Delta t\omega_i)/(1 + \theta\Delta t\omega_i)$ and, ω_i is the eigenvalue of the i^{th} mode of the system which is equal to $\omega_i = k_i/m_i$.

Since $\Delta t \geq 0$ and $\omega_i \geq 0$ and $0 \leq \theta \leq 1$, $\lambda < 1$. Therefore, stability is given if,

$$\lambda > -1$$

As a result, the stability requirement is:

$$(1/2)\omega_i\Delta t(1 - 2\theta) < 1 \quad (2.16)$$

For $\theta \geq 1/2$, the solution is unconditionally stable. But when $0 \leq \theta < 1/2$, stability is conditional on the following being satisfied:

$$\omega_i\Delta t < \frac{2}{1 - 2\theta} \quad (2.17)$$

If $\theta = 0$, the stability requires a time step limitation, i.e.

$$\Delta t < \frac{2}{\omega_i} \quad (2.18)$$

In the transient analyses presented in the next Chapter, $\theta = 0$, i.e. backward difference scheme, is adopted.

2.4 Discussion

In this chapter the numerical formulation for both steady state and transient heat transfer analysis used in this thesis was presented. This formulation was implemented into a MATLAB code for analysing 2D problems. Chapter 3 will describe the discretisation approaches investigated.

3 Discretisation approaches

This chapter describes the different approaches used to discretise the domain, which will be investigated in subsequent chapters. In all examples under consideration, a square domain is adopted.

3.1 Random point generation

For all discretisation approaches investigated, the domain was first populated with randomly generated nodes. To specify the number of nodes in the domain, two parameters are required. The first parameter is the density ρ_p of nodes placed in the domain, where $0 < \rho_p < 1$. If the density is low, this will result in a coarse distribution of nodes, with less nodes in the domain. The second parameter required is the minimum distance between the nodes m_d . These two parameters are used to control the number of nodes and uniformity of the point arrangement, as explained later in this chapter.

To ensure that nodes were appropriately placed to enforce the boundary conditions correctly, corner and boundary nodes were generated separately before the interior nodes. Furthermore, the spacing of nodes at the edge of the domain was less than in the interior of the domain, to ensure a well constructed Voronoi tessellation.

The number of nodes generated in the domain interior P_I is given as:

$$P_I = \frac{\ell^2 \rho_p}{m_d^2} \quad (3.1)$$

3 Discretisation approaches

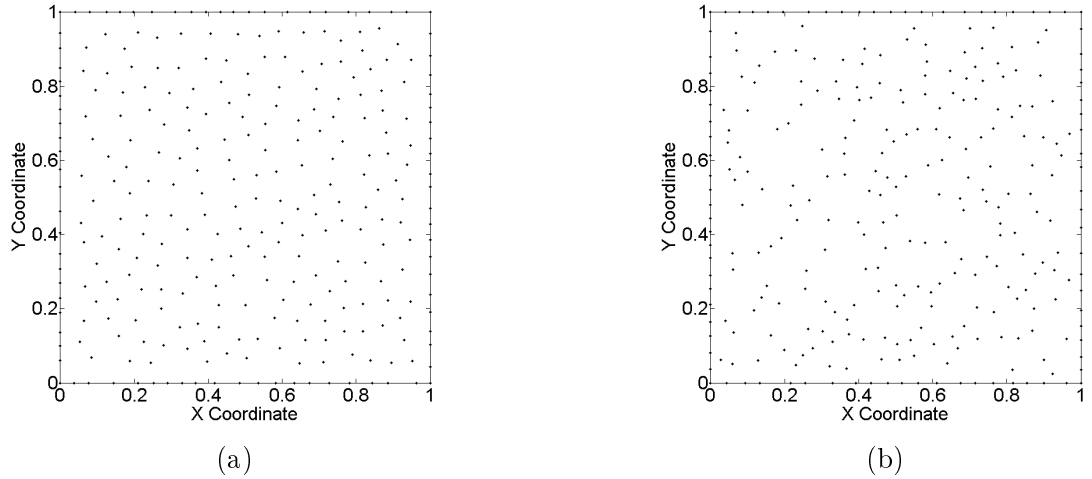


Figure 3.1: Point distribution method: (a) Quasi-uniform point distribution, (b) Non-uniform point distribution.

Here, ℓ is the side length of the square domain and m_d is the minimum distance between generated nodes.

For all analyses of the homogeneous medium, the number of nodes and side length were kept constant $P_1 = 200$, $\ell = 1$. Two levels of uniformity were considered to investigate the influence of the randomness of the nodes arrangements:

1. Quasi-uniform distribution, where $m_d = 0.05$ and $\rho_p = 0.5$ (Figure 3.1a).
2. Non-uniform distribution, where $m_d = 0.0316$ and $\rho_p = 0.2$ (Figure 3.1b).

For the generation of the nodes, random coordinates for each new node were generated by a MATLAB code. Before each new node was accepted, the distance to all existing nodes was first checked. If the distance was smaller than the minimum distance, the new node was rejected. Such a procedure requires a very large number of trial nodes to reach the desired point density. The maximum number of iterations was set equal to 1×10^7 .

3.2 Lattice generation

Following the population of the domain by randomly generated nodes, two discretisa-

3 Discretisation approaches

tion techniques are investigated for defining the lattice elements:

1. Delaunay triangulation
2. Voronoi tessellation

A Delaunay triangulation for a set of nodes is a triangulation such that no point lies inside the circumcircle of any of the triangles. Delaunay triangulation maximises the minimum angle of all the angles of the triangles in the triangulation. An example of the Delaunay triangulation, corresponding to the nodes shown in Figure 3.1a, is shown in Figure 3.2. The edges of the Delaunay triangles define the lattice elements. From this point forward this is called **Delaunay discretisation**.

Voronoi tessellation is the geometric dual of Delaunay triangulation, such that each of the Delaunay triangles' edges are bisected with a perpendicular line and the connection of these lines represent the Voronoi tessellation. Figure 3.3 shows the Voronoi polygons corresponding to the nodes in Figure 3.1a. The edges of these Voronoi polygons define an alternative set of lattice elements. From this point forward this is called **Voronoi discretisation**.

3.3 Cross-sectional area of lattice element

The lattice discretisation is completed by definition of the cross-sectional area of each of the lattice elements. Several definitions were investigated and presented in the following chapter.

3 Discretisation approaches

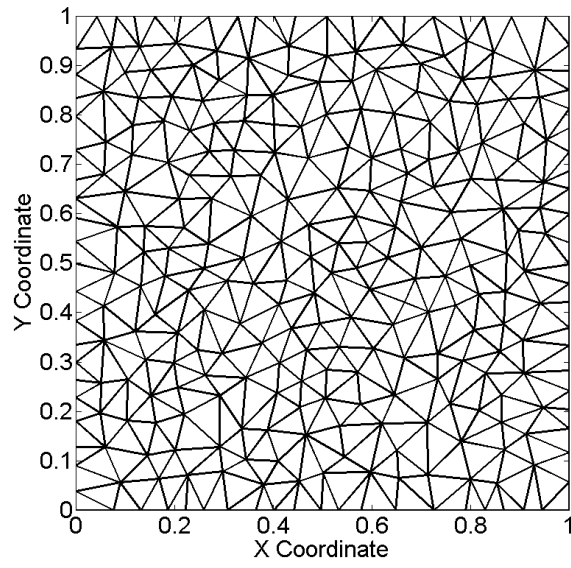


Figure 3.2: Delaunay domain discretisation for a set of nodes placed in the domain.

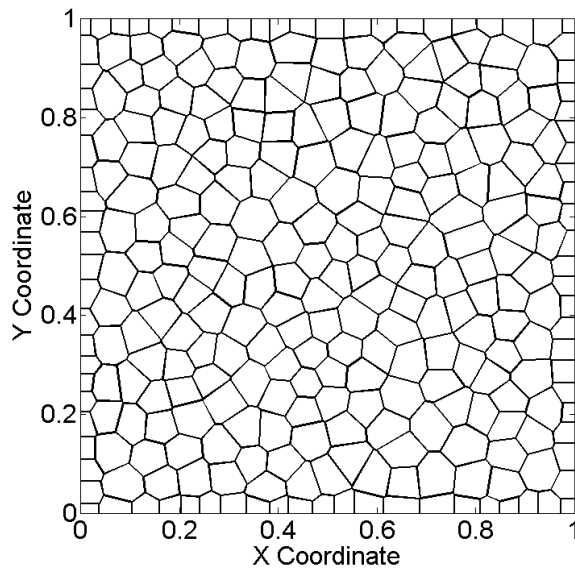


Figure 3.3: Voronoi domain discretisation for a set of nodes placed in the domain.

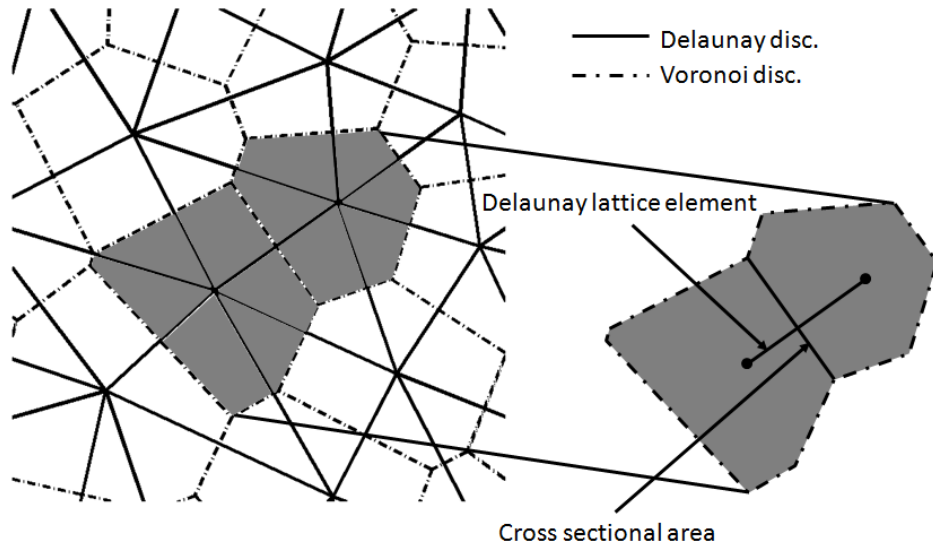


Figure 3.4: Voronoi scaling: Definition of the cross-sectional area of a lattice element determined by Delaunay discretisation.

3.3.1 Voronoi and Delaunay scaling

Two methods were used to define the cross-sectional area of the lattice elements for Delaunay and Voronoi discretisation. For the Delaunay discretisation, the cross-sectional area (assuming unit out-of-plane dimension) was defined as the corresponding length of the Voronoi polygon edge, as shown in Figure 3.4. This approach is called **Voronoi scaling** and was proposed by Bolander [2].

For the Voronoi discretisation, the cross-sectional area of the lattice element is determined by the length of the corresponding edge of the Delaunay triangle, as shown in Figure 3.5. This approach is called **Delaunay scaling**.

3.3.2 Average cross-sectional area

As a simpler alternative to the previous definitions, this approach assigns a constant cross-sectional area to all lattice elements and was used for both the Delaunay and

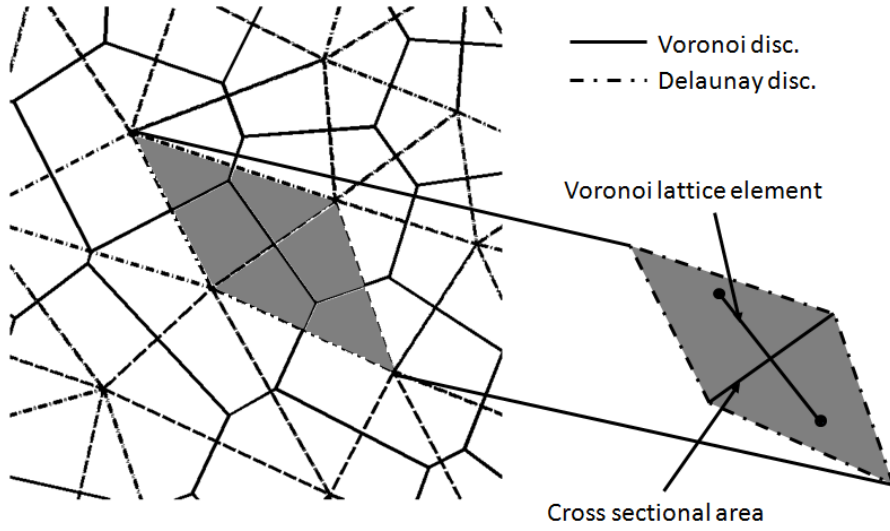


Figure 3.5: Delaunay scaling: Definition of the cross-sectional area of a lattice element determined by Voronoi discretisation.

Voronoi discretisation. For the Delaunay discretisation the constant cross-sectional area is determined as the average of all cross-sectional areas determined by the **Voronoi scaling**. The average cross-sectional area of all the lattice elements is given as:

$$\bar{A} = \frac{\sum_{i=1}^n A_i}{n} \quad (3.2)$$

where A_i is the area calculated from Voronoi scaling and n is number of lattice elements in the domain. A similar strategy is adapted for Voronoi discretisation.

3.3.3 Centroidal method

A further alternative approach was used to describe the cross-sectional area of lattice elements determined by the Delaunay discretisation. To understand this method, consider two neighbouring Delaunay triangles, Figure 3.6. First the triangles' centroids C_1 and C_2 are calculated. To calculate the cross-sectional area of element \overline{AB} the centroids

3 Discretisation approaches

are connected to the edges of the elements constructing the lines $\overline{AC_1}$, $\overline{AC_2}$, $\overline{BC_1}$ and $\overline{BC_2}$. The cross-sectional area will be presented by the summation of the triangles area ABC_1 and ABC_2 divided by the length of element \overline{AB} . Then multiplied by the specimen thickness (Eq 3.3, 3.4).

$$A^* = \frac{A_{ABC_1} + A_{ABC_2}}{L_{AB}} \quad (3.3)$$

$$E_a = A^*th \quad (3.4)$$

If element \overline{AB} lies on the edge of the specimen as shown in Figure 3.6, the cross-sectional area will be determined by the area of triangle ABC_1 divided by the length of \overline{AB} .

$$A^* = \frac{A_{ABC_1}}{L_{AB}} \quad (3.5)$$

$$E_a = A^*th \quad (3.6)$$

In summary four scaling techniques have been presented for determining the cross-sectional area of the lattice elements:

1. Voronoi scaling for Delaunay triangulation.
2. Delaunay scaling for the Voronoi tessellation.
3. Average cross-sectional area.
4. Centroidal method for the Delaunay triangulation.

3.4 Flux calculation

Once the system of equations have been solved to determine the temperature distribution in the lattice network, it is also helpful to be able to plot the nodal heat fluxes.

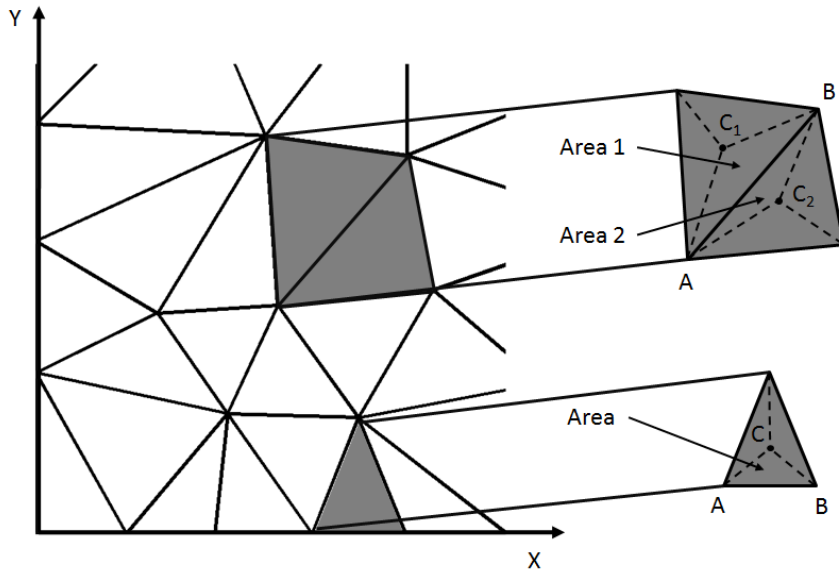


Figure 3.6: A section of Delaunay triangulation showing the cross-sectional area based on the centroidal method.

The method used follows that presented by Bolander [2] for a Delaunay discretisation. For a given point, first the associated Voronoi polygon is identified and a cutting plane is connected through the point. The left side of the plane is defined as positive and the right side as negative. The plane is rotated through an angle θ starting from 0 to 360° as shown in Figure 3.7. For each angle of rotation, a weighting factor R_i is calculated. There are three possible cases to be considered in calculating R_i for each angle of rotation:

1. $R_i = 1$ if both vertices of the Voronoi cell edge are located on the positive side of the cut.
2. $R_i = 0$ if both vertices of the Voronoi cell edge are located on the negative side of the cut.
3. $0 < R_i = a_i/b_i < 1$ if one of the Voronoi cell edges is located on the negative side and the other is located on the positive side. Here, b_i is the length of the Voronoi cell edge which is divided by the cut and a_i is the length of the Voronoi cell edge segment which is located on the positive side.

3 Discretisation approaches

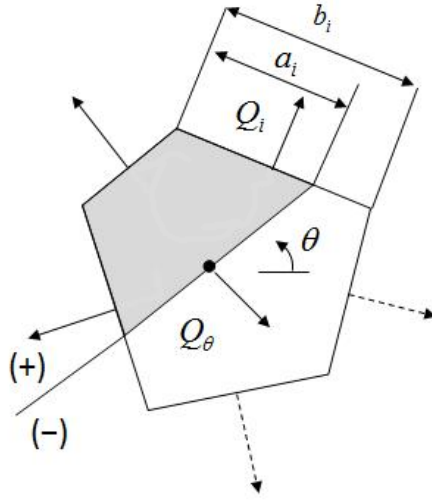


Figure 3.7: Flux calculation for a Delaunay element node.

After calculating the weighting factor, the net flow Q_θ for the cut face is calculated by,

$$Q_\theta = \sum_i^n R_i Q_i \quad (3.7)$$

where Q_i is the flux in a lattice element and n is the number of facets in the associated Voronoi cell.

The flux is calculated by dividing the net flow Q_θ by the area of the cut face A_θ ,

$$q_\theta = \frac{Q_\theta}{A_\theta} \quad (3.8)$$

This procedure will be repeated for each increment in θ . The maximum calculated q_θ is presented as the nodal flux.

3.5 Discussion

In this chapter the different lattice discretisation approaches were described. They were divided into two approaches, Delaunay discretisation and Voronoi discretisation.

3 Discretisation approaches

When using the Delaunay discretisation, lattice elements were represented by the edges of the Delaunay triangles. For Voronoi discretisation approach, the lattice elements were represented by the edges of the Voronoi polygons. The open Voronoi polygons on the edge of the domain were modified so that, where the end of an element was undefined, it was relocated onto the domain edge.

Moreover, various definitions for the lattice element cross-sectional area were described and the performance of these various methods are examined in the next chapter.

4 Results and discussions

4.1 Introduction

Until now, the lattice modelling approach and different lattice discretisation strategies were discussed in Chapters 2 and 3, respectively. In the present chapter, the capabilities of the different techniques are studied by analysing steady state and transient heat transfer problems for homogeneous and heterogeneous materials. The accuracy of the different discretisation strategies is assessed by comparing the numerical results with analytical solutions for several benchmark tests. The differences between the numerical and analytical solution are presented by several error norms.

4.2 Steady state analyses of a homogeneous square domain

In the first example, steady state heat transfer analyses of a homogeneous square domain are performed. The geometry of the domain is shown in Figure 4.1. The left and right hand side of the domain were subjected to temperatures of $T = 0$ and $T = 1$ as illustrated in Figure 4.1. The exact solution for this steady state heat transfer problem is

$$T_e(\mathbf{x}) = \frac{x}{\ell} \tag{4.1}$$

where x is the coordinate in horizontal direction, $T_e(x)$ is the temperature distribution in

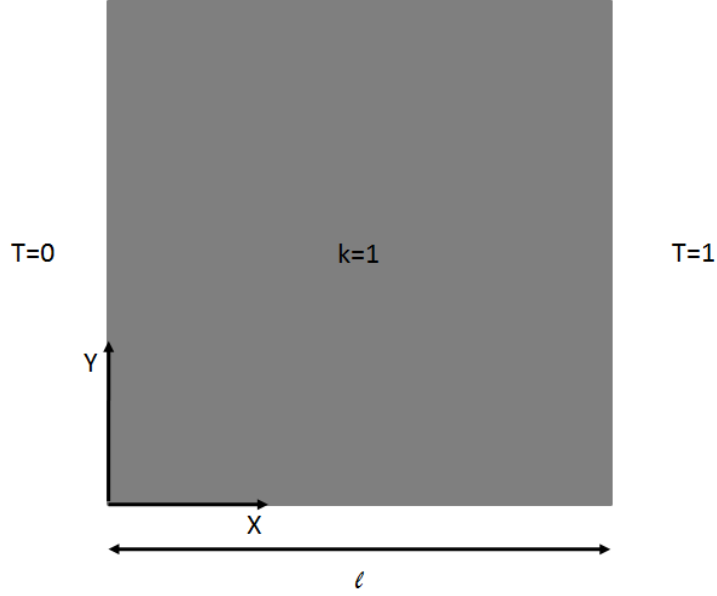


Figure 4.1: Domain geometry and boundary condition.

x -direction and ℓ is the length of the domain, which was chosen as $\ell = 1$ in all analyses.

The domain was assumed to be made of a homogeneous material with physical properties as shown in Table 4.1.

Table 4.1: Properties of the domain

Parameters	Values
ρ_p quasi-uniform	0.5
ρ_p non-uniform	0.2
m_d quasi-uniform	0.05
m_d non-uniform	0.0316
k	1
P_N	292

Initially, boundary conditions were imposed only at the left and right hand side of the domain according to the values $T = 0$ and $T = 1$ respectively. However, with this approach the exact solution could not be represented accurately because lattice elements close to the boundaries introduced an error into the numerical solution as discussed in Section 4.4. Therefore, the temperatures of all nodes located in a boundary layer along

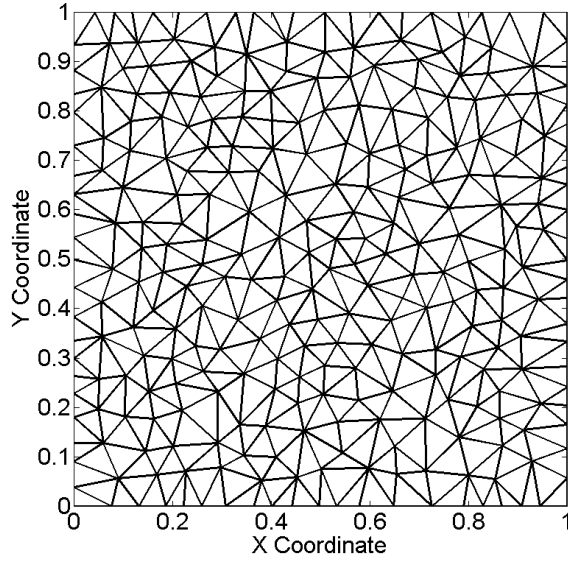


Figure 4.2: Delaunay domain discretisation based on a quasi-uniform point distribution.

the edges were prescribed according to the exact solution in Eq 4.1. The thickness of this boundary layer was set to 0.15ℓ .

All the analyses are based on Delaunay and Voronoi discretisations for two random point arrangements as shown in Figure 3.1a and 3.1b. The Delaunay and Voronoi discretisations for these random point generations are shown in Figure 4.2 to 4.5.

The numerical solutions associated with the two different discretisation techniques and the various techniques for calculating the cross-sectional area are presented.

4.2.1 Voronoi scaling

The results presented in this section were obtained for the two lattices shown in Figures 4.2 and 4.4, which are based on Delaunay discretisation and Voronoi scaling to determine the cross-sectional area of the lattice element (Section 3.3.1). The results of the numerical analyses for the uniform and non-uniform lattices are shown in Figure 4.6 and 4.7, respectively, in the form of the temperature distribution along the x-

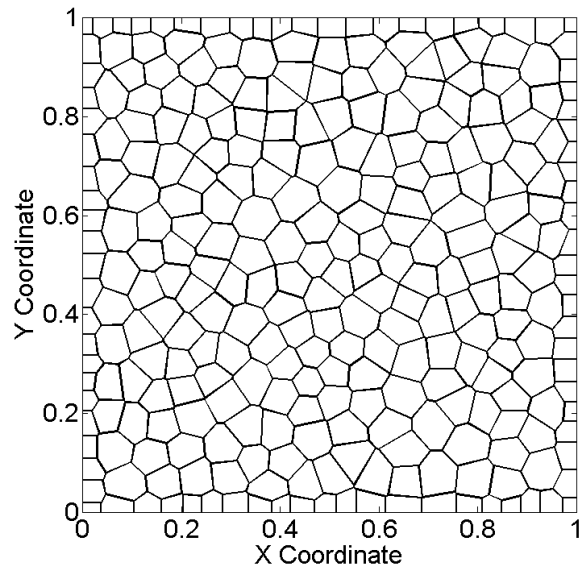


Figure 4.3: Voronoi domain discretisation based on a quasi-uniform point distribution.

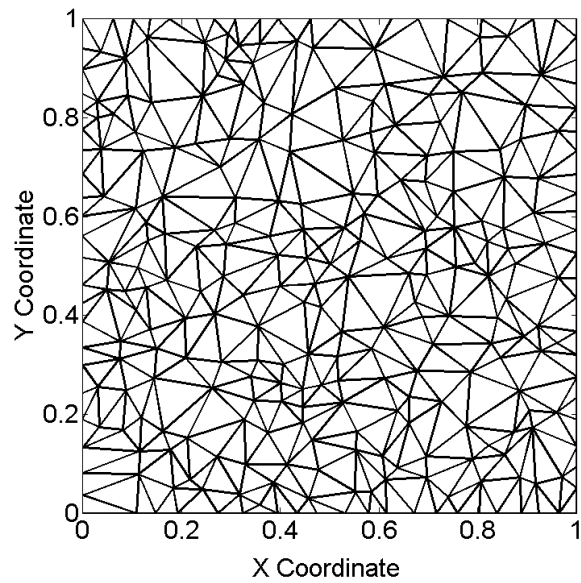


Figure 4.4: Delaunay domain discretisation based on a non-uniform point distribution.

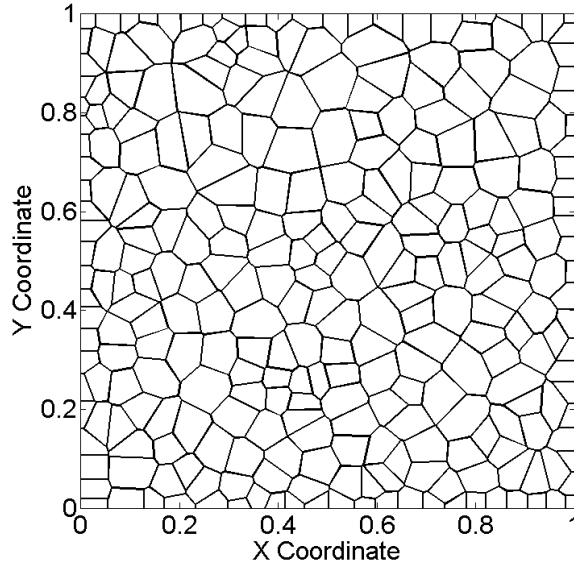


Figure 4.5: Voronoi domain discretisation based on a non-uniform point distribution.

direction in the middle of the domain ($y = 0.5$). The agreement between the numerical and analytical results appears to be very good. To investigate the possible difference between the two solutions in more detail, the results are evaluated by the error norms which are defined in Eq. (4.2) and (4.3):

$$L_1 = \sum \frac{|T_{a_i} - T_{n_i}|}{|T_{a_i}| P_N} \quad (4.2)$$

$$L_2 = \frac{\sum (T_{a_i} - T_{n_i})^2}{\sum T_{a_i}^2} \quad (4.3)$$

Here, T_a is the analytical solution and T_n is the numerical solution.

For the quasi-uniform lattice, the errors computed from the analytical and numerical solutions are $L_1 = 5.6425 \times 10^{-16}$ and $L_2 = 6.3704 \times 10^{-16}$. For the non-uniform lattice, the error norms are $L_1 = 3.2273 \times 10^{-16}$ and $L_2 = 5.1397 \times 10^{-16}$.

The small error norms indicate that the agreement between the results is very good and that, even for a non-uniform lattice, the lattice approach performed very well.

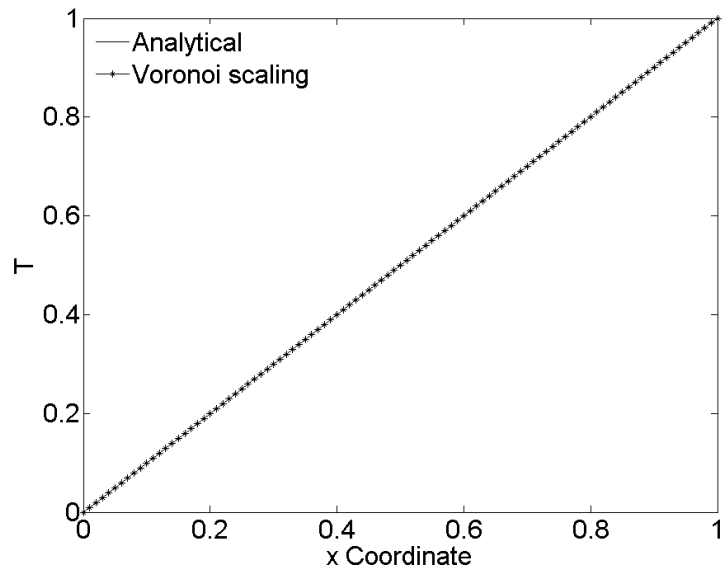


Figure 4.6: Comparison of numerical and analytical solution for a quasi-uniform lattice.

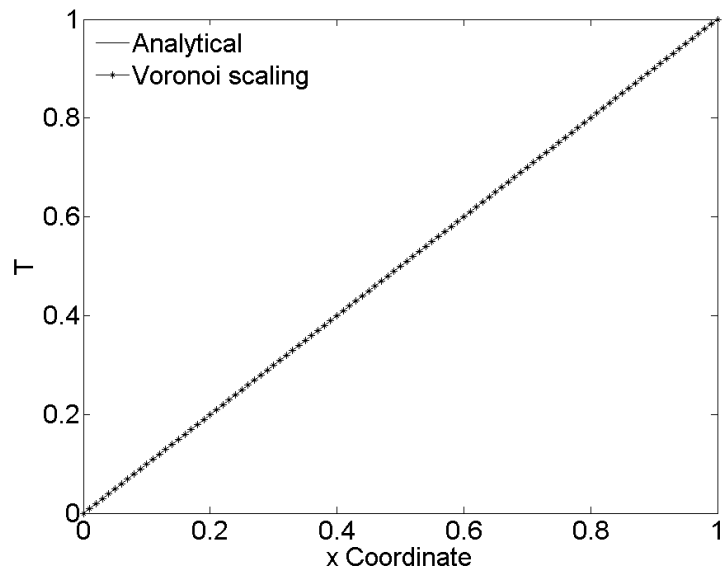


Figure 4.7: Comparison of numerical and analytical solution for a non-uniform lattice.

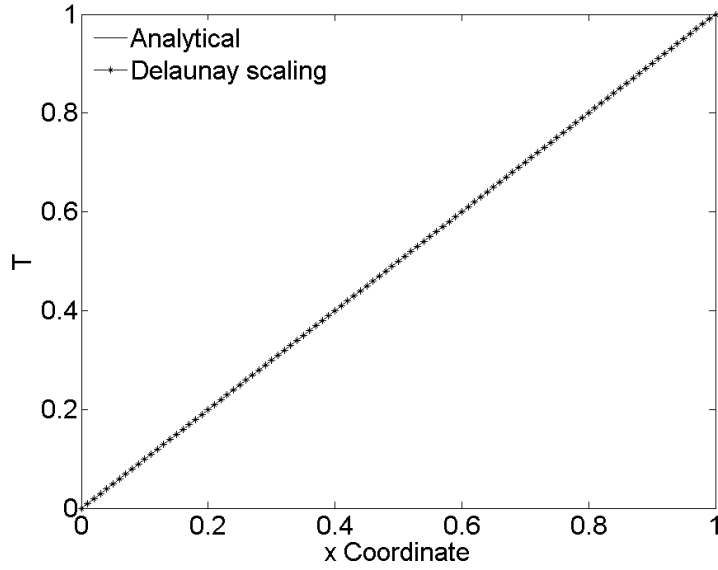


Figure 4.8: Comparison of numerical and analytical solution for a quasi-uniform lattice.

4.2.2 Delaunay scaling

The second approach to determine the cross-sectional area of the lattice elements is the Delaunay scaling (Section 3.3.1). For the Delaunay scaling, the lattice elements are generated by the Voronoi discretisation. This scaling approach was tested for a uniform and a non-uniform point distribution (Figures 4.3 and 4.5). Again, the results are presented in the form of the temperature distribution along the x-direction in the middle of the domain ($y = 0.5$) in Figures 4.8 and 4.9. In addition, the error norms were computed. For the uniform mesh (Figure 4.3), $L_1 = 9.0141 \times 10^{-16}$ and $L_2 = 1.0594 \times 10^{-15}$. For the non-uniform mesh (Figure 4.5) the nodal temperature error norms were $L_1 = 3.6698 \times 10^{-15}$ and $L_2 = 7.9849 \times 10^{-15}$. Similar to the Voronoi scaling, the Delaunay scaling results in a very accurate approximation of the analytical

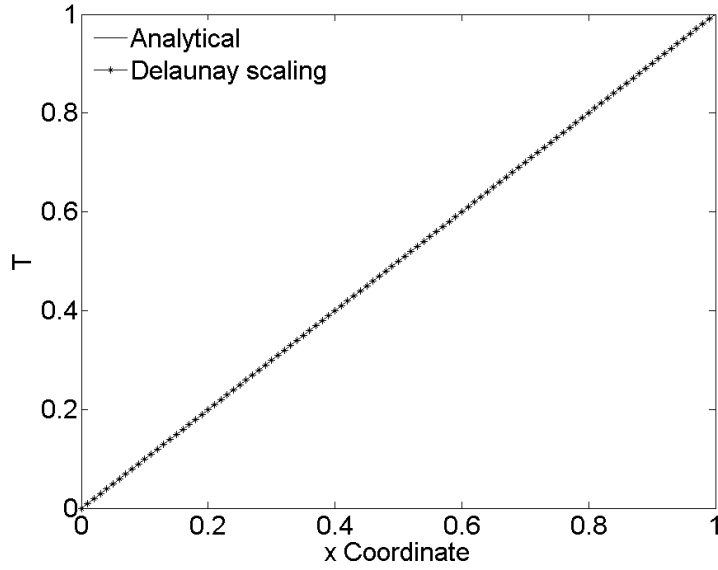


Figure 4.9: Comparison of numerical and analytical solution for a non-uniform lattice.

solution.

4.2.3 Centroidal scaling

The third scaling approach is based on the centroidal method, which was described in Section 3.3.3. This scaling method applies only to lattices generated by the Delaunay discretisation. The temperature distribution obtained from the numerical solution with this scaling approach is compared to the analytical solution in Figure 4.10 and 4.11 for the quasi-uniform and non-uniform lattice, respectively. For the quasi-uniform mesh, the error norms were determined to $L_1 = 0.0248$ and $L_2 = 0.01436$. On the other hand, for the non-uniform mesh the error norms were determined to $L_1 = 0.027487$ and $L_2 = 0.017975$. It can be seen that this centroidal scaling approach does not result in a

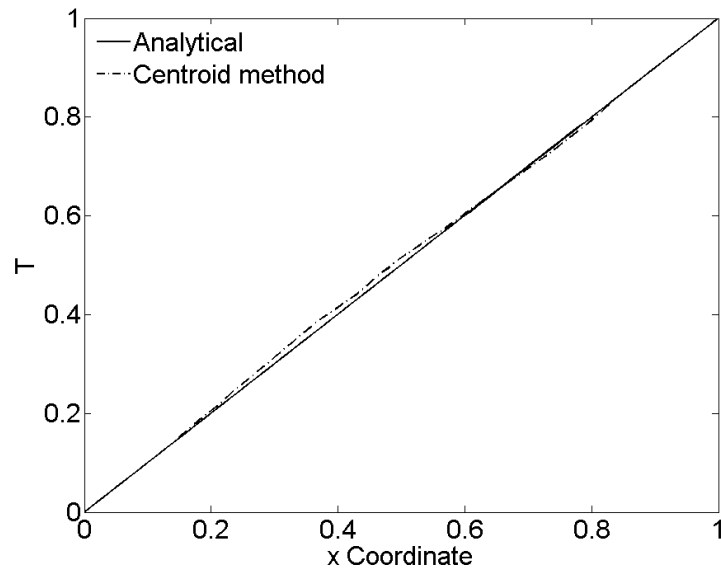


Figure 4.10: Comparison of numerical and analytical solution using the centroidal method for a quasi-uniform lattice.

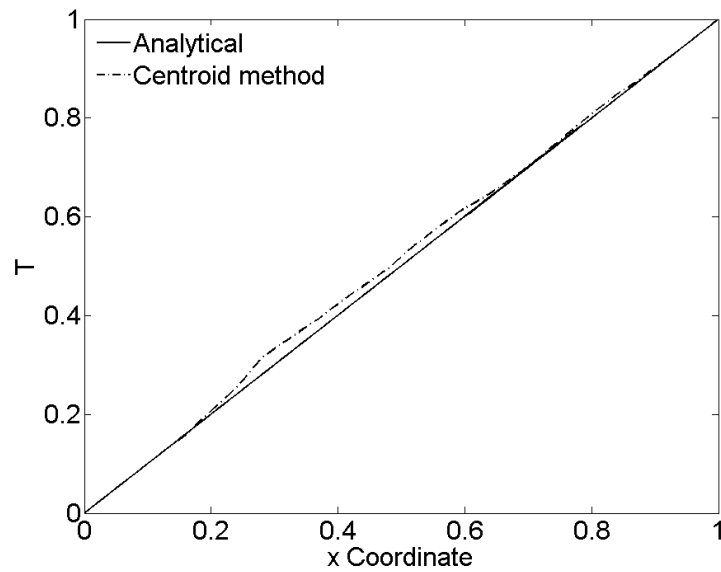


Figure 4.11: Comparison of numerical and analytical solution using the centroidal method for a non-uniform lattice.

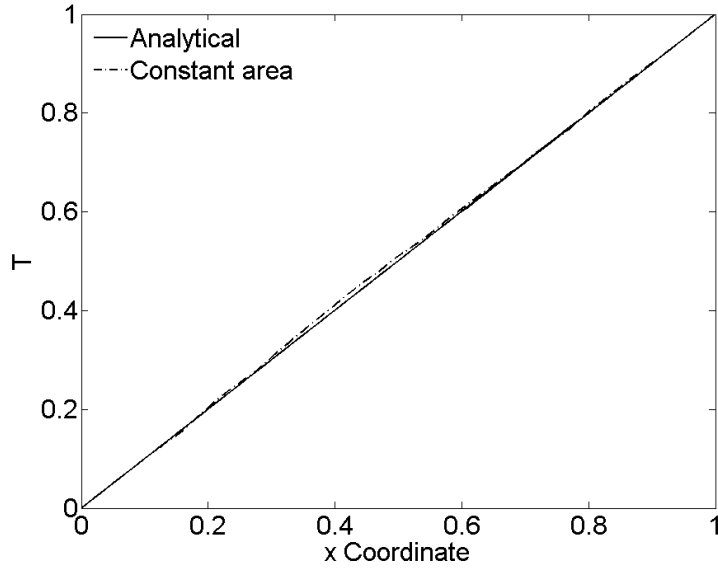


Figure 4.12: Comparison of numerical and analytical solution using a constant cross-sectional area for a quasi-uniform lattice based on the Delaunay discretisation.

good approximation of the analytical solution.

4.2.4 Constant cross-sectional area

In the last method, the cross-sectional area of the lattice elements is set to a constant value, which is chosen to be the average cross-sectional area of all lattice elements in the domain (Section 3.3.2). This approach is applied to the Delaunay and Voronoi discretisation for a non-uniform and a quasi-uniform mesh. For the Delaunay discretisation, the results obtained from the numerical analysis with a constant cross-sectional area are shown in the form of the temperature distribution in x-direction in the middle of the specimen ($y = 0.5$) in Figures 4.12 and 4.13 for the quasi-uniform and non-uniform mesh, respectively. In addition, the two error norms are determined for the two meshes. For the quasi-uniform mesh, $L_1 = 0.009792$ and $L_2 = 0.015180$. For the non-uniform

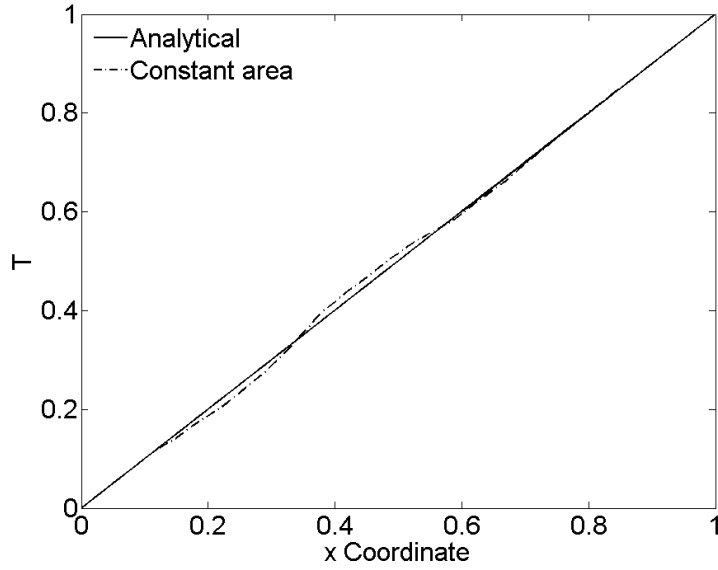


Figure 4.13: Comparison of numerical and analytical solution using a constant area for a non-uniform lattice based on the Delaunay discretisation.

mesh, $L_1 = 0.009241$ and $L_2 = 0.012967$.

For the Voronoi discretisation, the temperature distributions are shown in Figures 4.14 and 4.15. The error norms are determined to $L_1 = 0.005337$ and $L_2 = 0.006852$ for the quasi-uniform mesh and $L_1 = 0.008688$ and $L_2 = 0.0012163$ for the non-uniform mesh. The results show that the use of a constant cross-section does not lead to a good approximation of the analytical solution.

The poor results using both this scaling technique and the centroidal method indicates that correct scaling of the cross-sectional area is critical if the lattice approach is to be successful.

4.3 Transient analyses

In this section, transient analyses based on the theory described in Section 2.3.2 are performed for the square domain introduced in the previous section. It was observed that

4 Results and discussions

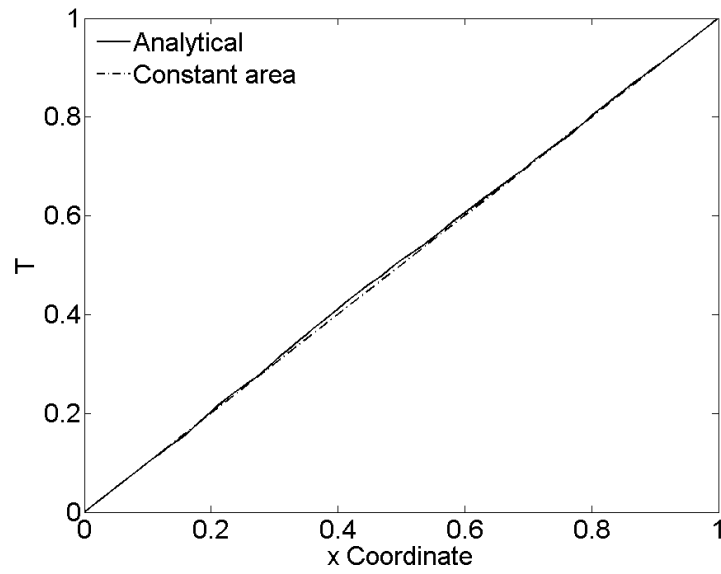


Figure 4.14: Comparison of numerical and analytical solution using a constant area for a uniform lattice based on the Delaunay discretisation.

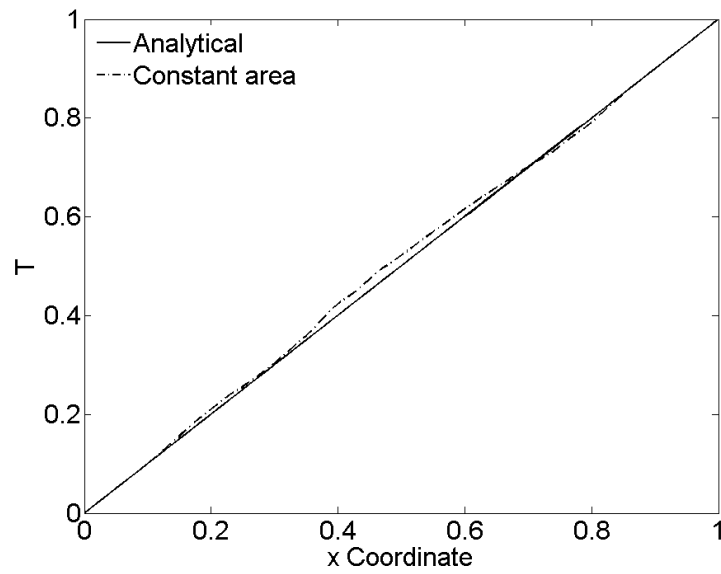


Figure 4.15: Comparison of numerical and analytical solution using a constant area for a non-uniform lattice based on the Voronoi discretisation.

4 Results and discussions

only Delaunay and Voronoi scaling result in an accurate approximation of the analytical solutions for the steady-state analysis performed. Therefore, these two approaches are used in this section for the transient analyses based on the θ -method described in Section 2.3.2. Two benchmark tests were used to study the performance of the lattice approach for transient analyses. The same quasi-uniform and non-uniform nodes distribution is used for the discretisation of the domain. For both tests, the properties of the lattice elements were chosen according to the values shown in Table 4.2.

Table 4.2: Properties of the domain

Parameters	Values
ρ	1
C	1
k	1
θ	0.9
t	1.2
Δt	0.001

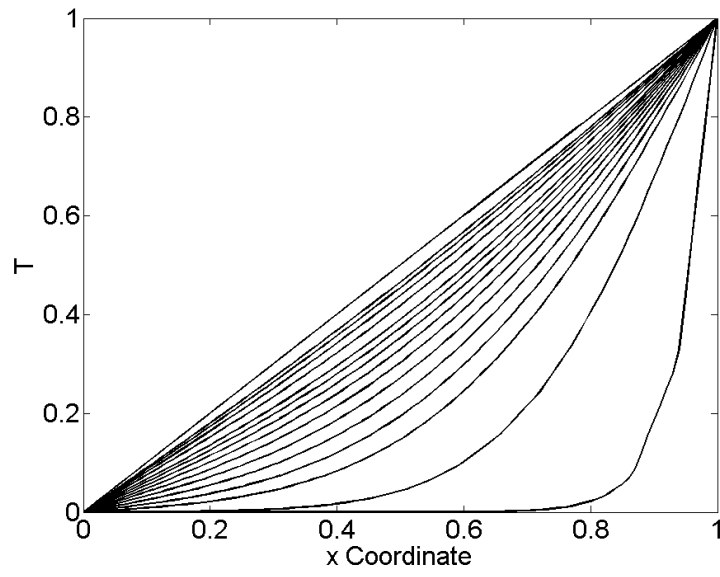
where, ρ is the element density, C is the specific heat capacity of the element, t is the total time of the analyses and Δt is the increments of each time step.

The two benchmark tests differ in their initial conditions. In the first benchmark test, the initial condition for all nodes was $T = 0$ at time $t = 0$. For $t > 0$, the temperatures at the nodes on the left and right hand side of the domain were set to 0 and 1, respectively. The first set of analyses was performed using the Delaunay discretisation and Voronoi scaling for the cross-sectional areas. The results are shown as the temperature distribution along the x -axis in the middle of the specimen ($y = 0.5$) in Figure 4.16 for the quasi-uniform and non-uniform point distribution.

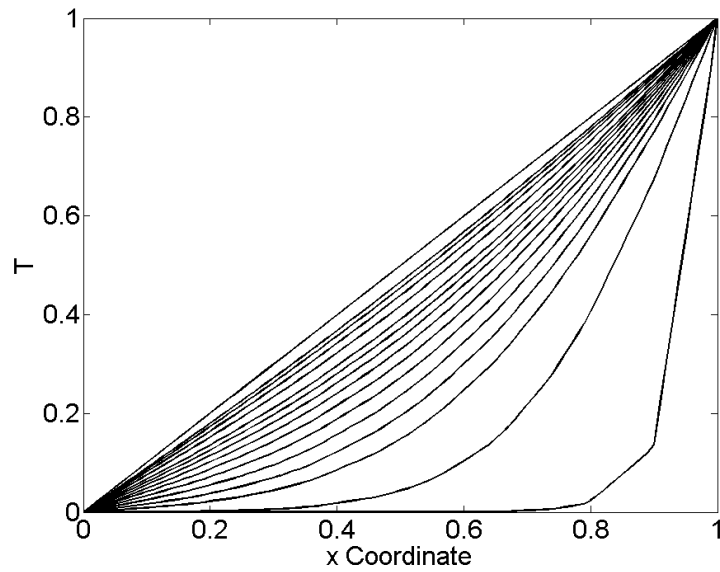
The behaviour is very similar for both the quasi-uniform lattice and the non-uniform lattice. With increasing time, the temperature in the domain increases until the linear temperature distribution, which is the steady-state limit presented in the previous section, is reached.

The second set of analyses was performed using the Voronoi discretisation with Delau-

4 Results and discussions



(a)



(b)

Figure 4.16: Temperature distribution along in the x -direction for $y = 0.5$ for time steps varying from 0 to 1 using a (a) quasi-uniform lattice and (b) non-uniform lattice based on the Delaunay discretisation.

may scaling for the determination of the cross-sectional areas. The results obtained for both quasi-uniform and the non-uniform mesh is shown in Figure 4.17.

Again, the behaviour is very similar for both the quasi-uniform lattice and the non-uniform lattice. With increasing time, the temperature in the domain increases until the linear temperature distribution, which is the steady-state limit from the example in the previous section, is reached. The first benchmark test gave qualitatively good results. However, the performance of the lattice model cannot be assessed quantitatively with this test. Therefore, a second benchmark test is carried out, which allows for the comparison of the numerical solution with an analytical one. The choice of this test is motivated by the study of Bolander [2]. In this test, the initial conditions of the problem are given as

$$T(x, y, t = 0) = \sin \frac{\pi x}{\ell} \quad (4.4)$$

The analytical solution is

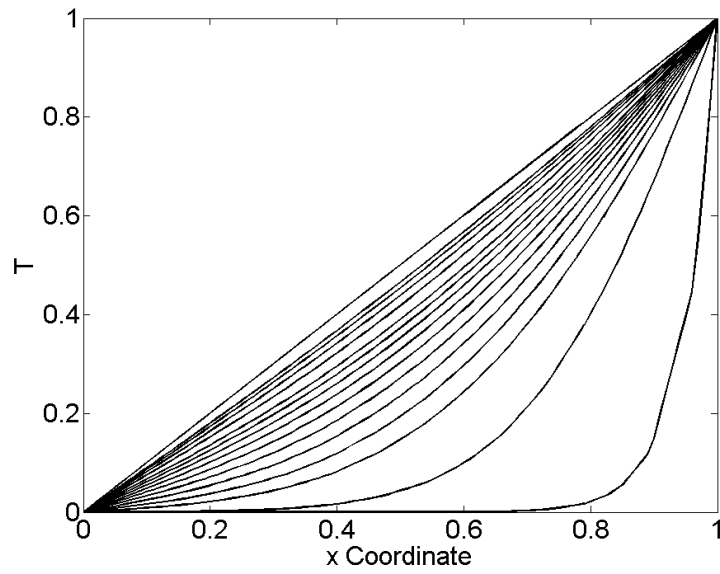
$$T(x, t) = \sin \left(\frac{\pi x}{\ell} \right) e^{-\frac{\pi^2 t}{\ell^2}} \quad (4.5)$$

Again, the position of the lattice elements is determined by the Delaunay and Voronoi discretisation. Furthermore, the cross-sectional areas of the lattice elements were determined using Voronoi and Delaunay scaling. The numerical solution of the temperature distribution in the x -direction for a section at a distance of 0.5 from the Y axis is compared to the analytical solution in Figure 4.18. The numerical and analytical results agree well.

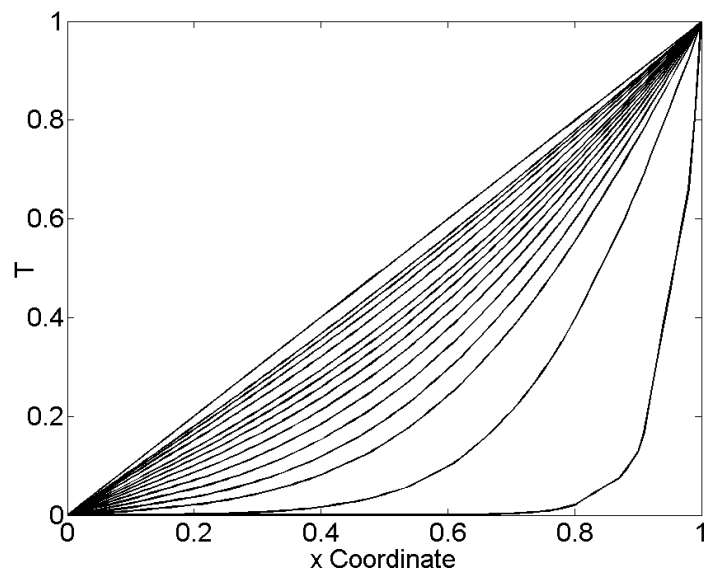
4.4 Effect of boundary layer on accuracy

This section discusses the treatment of the boundary conditions used in the analyses. In Section 4.2 it was explained that the boundary conditions are applied according to the analytical solution with in a distance of the boundary. This distance was chosen in relation to the lengths of the lattice elements. This special treatment of the boundary

4 Results and discussions



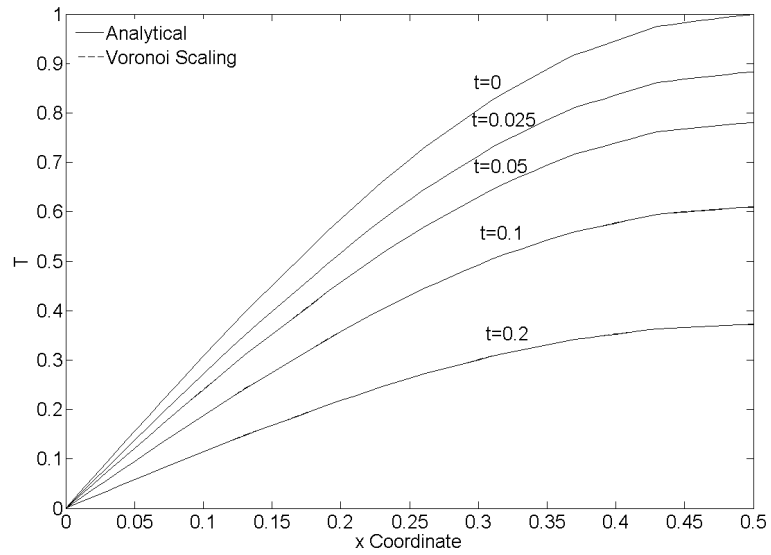
(a)



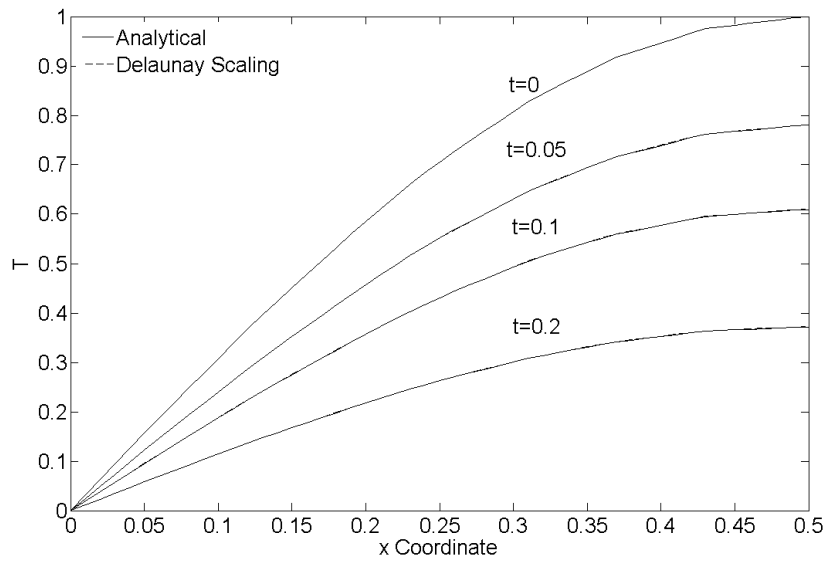
(b)

Figure 4.17: Temperature distribution along the x -direction for $y = 0.5$ for the (a) quasi-uniform lattice (b) non-uniform lattice based on the Voronoi discretisation.

4 Results and discussions



(a)



(b)

Figure 4.18: Transient analyses of the domain with comparison to the analytical solution: (a) Delaunay discretisation, (b) Voronoi discretisation.

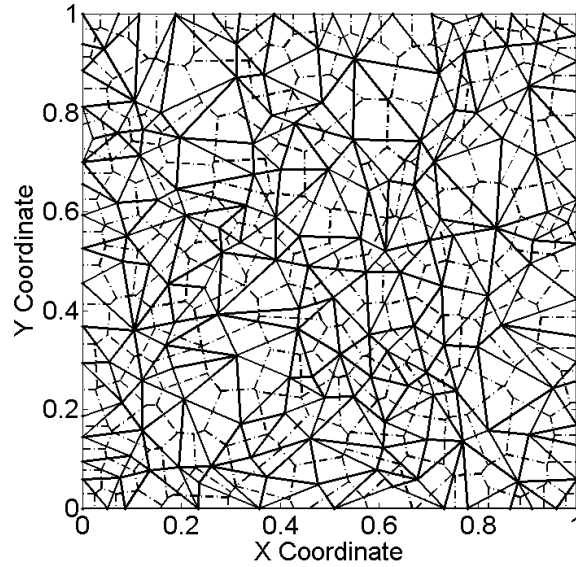


Figure 4.19: Delaunay and Voronoi domain discretisation based on a non-uniform point distribution.

is required since otherwise the numerical solution might deviate considerably from the analytical one. The influence of the boundary layer is illustrated by the steady state heat transfer problem analysed in Section 4.2. The domain geometry and boundary conditions are shown in Figure 4.1. The results, obtained for a lattice based on Delaunay discretisation and Voronoi scaling, are shown in Figure 4.19. The domain is assumed to be made of a homogeneous material with physical properties as shown in Table 4.3.

Table 4.3: Physical properties of the domain.

Parameters	Values
ρ_p	0.3
k	1
m_d	0.05
P_N	175

Three different treatments of the boundary conditions are studied. In the first approach, no boundary frame is used. Boundary conditions are presented only on the

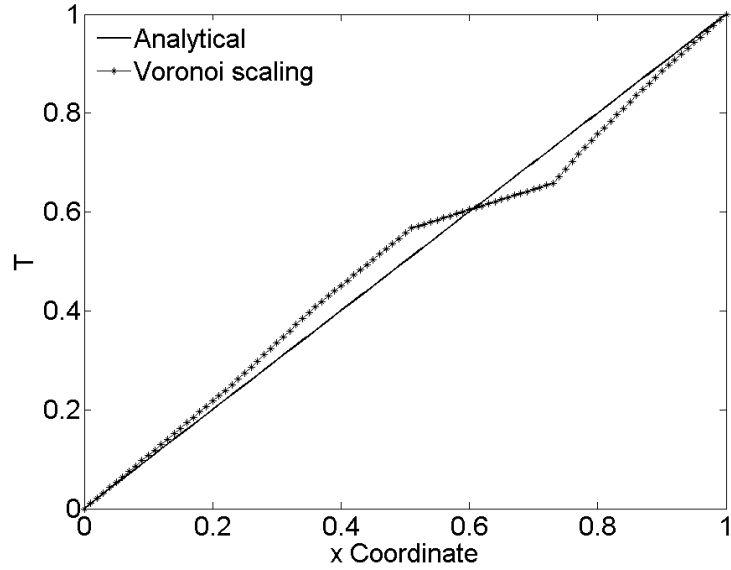


Figure 4.20: Comparison of numerical and analytical solution at $y = 0$. The boundary conditions are described only on the left and right of the domain.

left and right side of the domain. The results obtained from the numerical analysis are compared to the analytical solution in Figure 4.20.

The second approach is based on the introduction of a frame along the edge of the specimen, in which the boundary conditions are applied according to the analytical solution. Two analyses with different frame thickness are performed. In the first analysis, the frame thickness is set to 0.1ℓ . The results obtained from the numerical analysis are compared to the analytical solution in Figure 4.21.

In the second analysis, the frame thickness is set to 0.2ℓ . The results obtained from the numerical analysis are compared to the analytical solution in Figure 4.22.

In Figure 4.20 to 4.22, it can be seen that the introduction of the frame has a strong influence on the results. For the analysis without the frame and a frame thickness of 0.1ℓ , the numerical results differ strongly from the analytical results. Only for a frame of 0.2ℓ a good approximation of the analytical result is obtained. The thickness of the

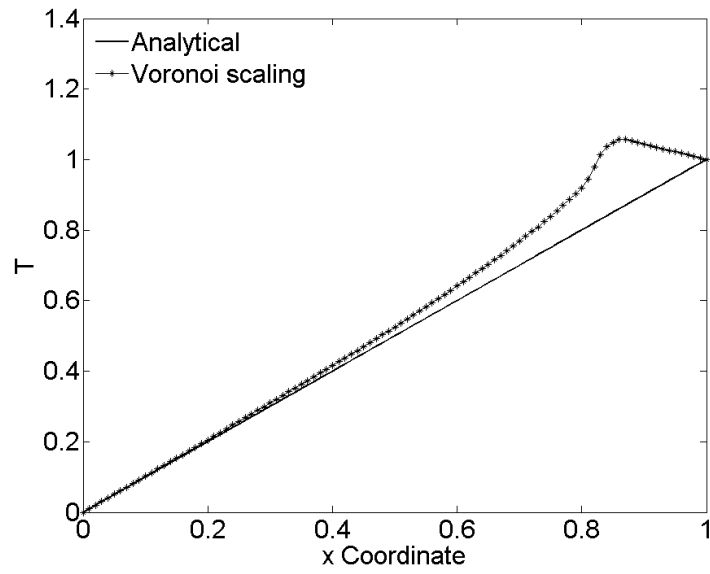


Figure 4.21: Comparison of numerical and analytical solution at $y = 0.3$. The boundary conditions are described as a frame with the thickness of 0.1ℓ .

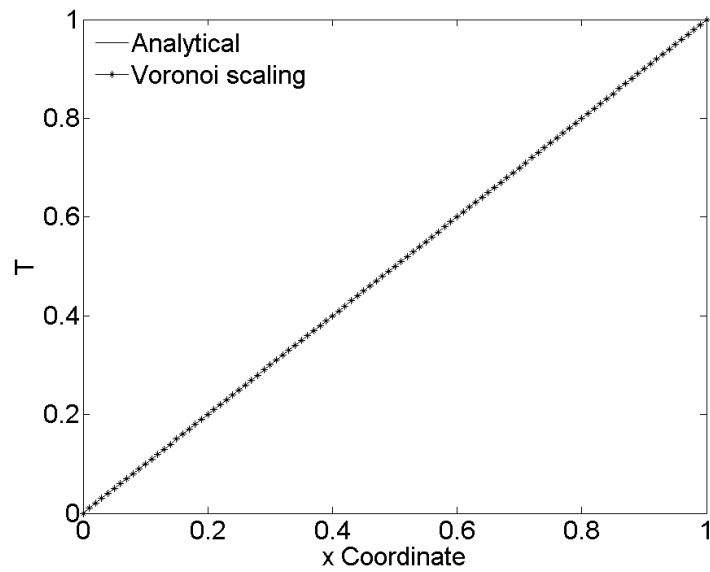


Figure 4.22: Comparison of numerical and analytical solution at $y = 0.3$. The boundary conditions are described as a frame with the thickness of 0.2ℓ .

Table 4.4: Properties of the domain with an inclusion

Parameters	Values
ℓ	1
r	0.01
k_1	1
k_2	1×10^{-15}
N_p	2728

frame, which results in a good approximation of the analytical solution, depends on the length of the elements. If the density of the mesh is changed, the thickness of boundary layer should be adjusted to cover all nodes connected to the Voronoi cell at the domain boundary. Thus, the lattice approach result only in exact solutions for the Voronoi cells inside the domain.

4.5 Steady state analyses of homogeneous domain with isolated inclusion

In the previous two sections, steady state and transient analyses were performed for quasi-uniform and non-uniform lattices, different discretisation and different scaling approaches. All of these analyses were performed for a homogeneous domain. In this section, the lattice approaches are applied to heterogeneous materials.

The benchmark test considered here is a square domain with an inclusion of a radius of $r = \ell/100$ in the centre. The input parameters for the analyses are listed in Table 4.4, where k_1 is the conductivity of the domain outside the inclusion and k_2 is the conductivity of the inclusion.

Again, the Delaunay and Voronoi discretisations were applied to determine the positions of the lattice elements. Furthermore, the cross-sectional areas of the lattice elements were determined by Delaunay and Voronoi scaling. However, the point distribution for

4 Results and discussions

the different discretisations was different. Within the inclusion the distance between nodes is smaller than outside the inclusion. This results in a denser lattice inside the inclusion. The lattice mesh is shown in Figure 4.23. The boundary condition was applied only on the left and right edges of the domain, because in these analyses the main aim is to study the inside of the domain where the inclusion is located.

The first analysis was performed using the Delaunay discretisation and Voronoi scaling. The temperature distribution in the x -direction for $y = 0.5$ is shown in Figure 4.24.

Figure 4.24b shows the temperature distribution across the inclusion and the effect of the very low thermal conductivity of the inclusion compared to the surrounding material.

As part of the post-processing, the nodal flux was calculated. The method of calculating the nodal flux was presented in Section 3.4. The analytical solution for the flux within the domain with the inclusion was used earlier by Bolander [2] to assess the accuracy of lattice approaches. The analytical solution is expressed in polar form as

$$q = \sqrt{\left(\frac{r}{x}\right)^4 + 1 - 2\cos 2\theta \left(\frac{r}{x}\right)^2} \quad (4.6)$$

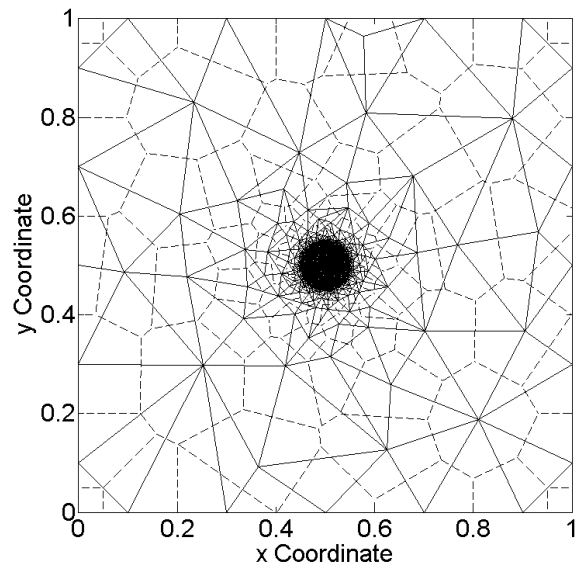
where r is the radius and θ is the angle of a polar co-ordinate system with its origin in the centre of the inclusion.

The flux obtained with the Delaunay discretisation compared to the analytical solution is shown in Figure 4.25. It can be seen that there is no flux on the left and right sides of the isolated inclusion, but consequently concentration of the flux at the top and bottom.

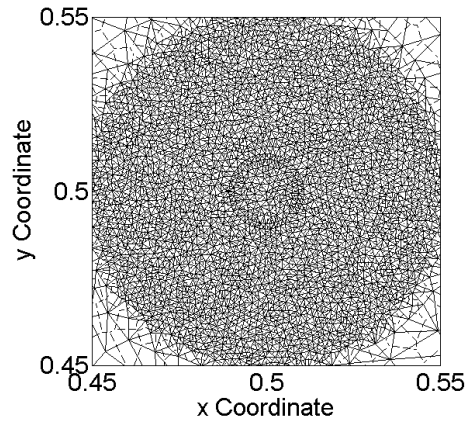
4.6 Discussion

In this chapter steady state and transient analyses were performed with two discretisation approaches based on Delaunay triangulation and Voronoi tessellation, respectively. It was

4 Results and discussions



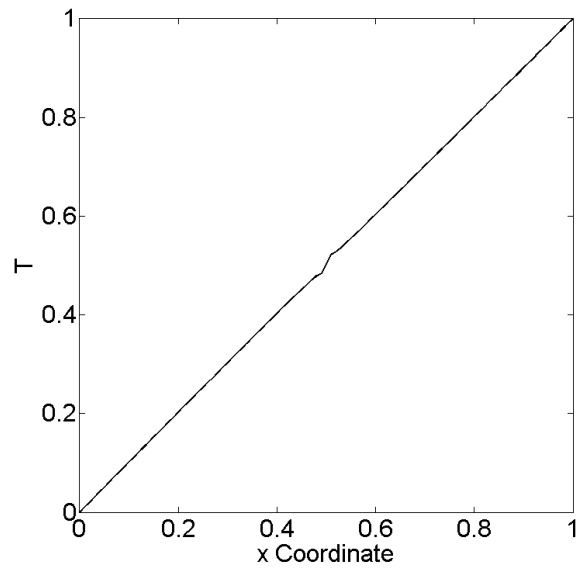
(a)



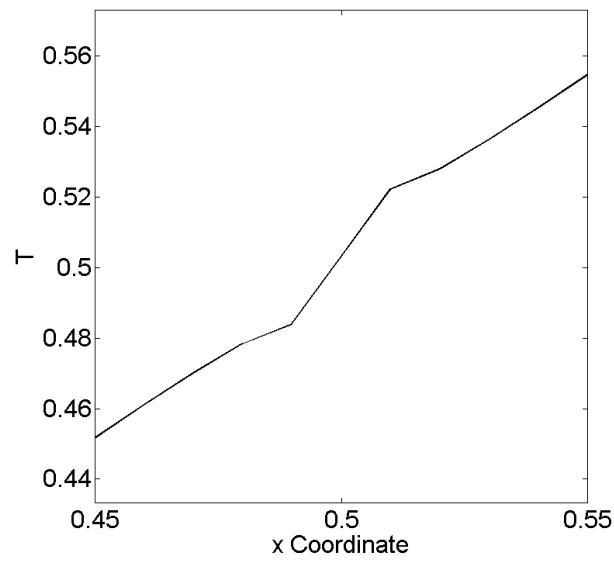
(b)

Figure 4.23: Domain discretisation with an inclusion: (a) The domain discretisation (b) The discretisation of the inclusion.

4 Results and discussions



(a)



(b)

Figure 4.24: Temperature distribution along the x-direction for $y = 0.5$: (a) The entire specimen (b) Detail around the inclusion.

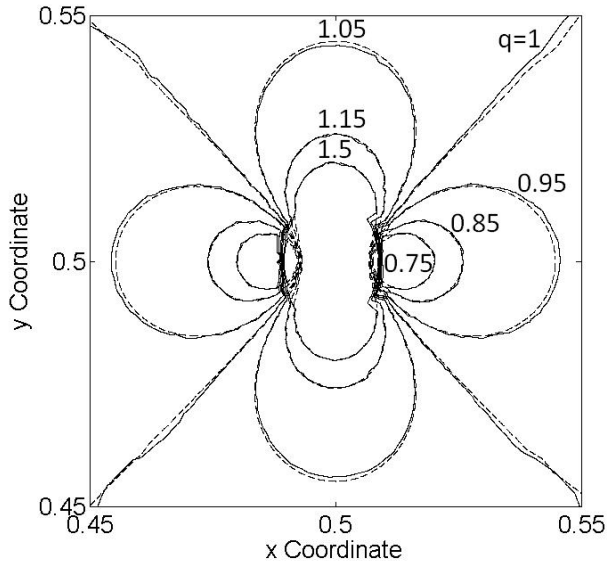


Figure 4.25: Flux around an inclusion obtained by the Delaunay discretisation. The solid and dashed lines represent the numerical and analytical solution, respectively.

shown that the lattice approach performed very well for both quasi-uniform and transient analyses and for both quasi-uniform and non-uniform lattices, if the correct scaling of the cross-sectional area is adopted. Four different methods for determining the cross-sectional areas of the lattice elements were investigated. It was shown that the use of cross-sectional areas determined by Voronoi and Delaunay scaling results in numerical solutions which approximate well the analytical solutions. However, if the cross-sectional areas are determined by the centroidal method or if a constant cross-sectional area is used, the lattice approach fails to represent the analytical solutions exactly.

Transient analyses using the Delaunay and Voronoi discretisation with Voronoi and Delaunay scaling, respectively, showed that accurate solutions are obtained with the θ -Method.

Furthermore, the inclusion problem demonstrated that the lattice approach performs well for heterogeneous material. The post-processing of the flux proved a useful technique

4 Results and discussions

to visualize results and demonstrated that the numerical and analytical solutions agree well.

5 Conclusions and suggestions for future studies

5.1 Conclusions

In the work presented, a 2D lattice approach was investigated for solving heat transfer problems. Two alternative discretisation were implemented. It was shown that the performance of lattice approach was dependent on the scaling of the cross-sectional areas of the lattice elements. Four scaling methods were investigated:

1. Voronoi scaling for the lattice generated from the Delaunay triangulation.
2. Delaunay scaling for the lattice generated from the Voronoi tessellation.
3. Centroidal method.
4. Constant average area method.

Both the Voronoi and Delaunay scaling methods enabled the lattice approach to accurately reproduce analytical solutions. This is not the case for the other two scaling methods.

In addition to steady state heat transfer analysis across a square domain with a homogeneous material, the effect of an isolated inclusion was investigated. A post-processing procedure was investigated in order to visualise the non-uniform heat flux. Once again the lattice approach with Voronoi and Delaunay scaling accurately represented the analytical solution.

5 Conclusions and suggestions for future studies

The lattice modelling was also extended to transient heat transfer. Both methods of discretisation allowed for an accurate representation of the analytical solution when Voronoi and Delaunay scaling was adopted.

5.2 Suggestions for future studies

The present work is restricted to two-dimensions. A natural extension of the work would be to three-dimensions, thereby providing wide application of the technique.

To date lattice models have been successfully applied to the mechanical behaviour of elastic and fracturing materials of heterogeneous materials. A next step could be to combine heat transfer modelling presented in this thesis with the lattice modelling of mechanical behaviour, thereby enabling thermo-mechanical behaviour of fracturing heterogeneous materials to be considered and to investigate the effect of fracture on the thermal response.

This could be further extended to the coupling of the mechanical response with other transport phenomena.

Bibliography

- [1] CALFEM a finite element toolbox to matlab, http://www.aaue.dk/bm/fem_ld/pdfcalfem.pdf, 1999.
- [2] J. E. Bolander and S. Berton. Simulation of shrinkage induced cracking in cement composite overlays. *Cement & Concrete Composites*, 26(7):861–871, 2004.
- [3] J. E. Bolander and S. Saito. Fracture analysis using spring networks with random geometry. *Engineering Fracture Mechanics*, 61:569–591, 1998.
- [4] J. E. Bolander and N. Sukumar. Irregular lattice model for quasistatic crack propagation. *Physical Review B*, 71:094106:1–12, 2005.
- [5] G. Chatzigeorgiou, V. Picandet, A. Khelidj, and G. Pijaudier-Cabot. Coupling between progressive damage and permeability of concrete: analysis with a discrete model. *International Journal for Numerical and Analytical Methods in Geomechanics*, 29(10):1005–1018, 2005.
- [6] A. Delaplace, G. Pijaudier-Cabot, and S. Roux. Progressive damage in discrete models and consequences on continuum modelling. *Journal of the Mechanics and Physics of Solids*, 44(1):99–136, 1996.
- [7] P. Grassl. A lattice approach to model flow in cracked concrete. *Cement & Concrete Composites*, 31(7):454–460, 2009.

Bibliography

- [8] P. Grassl and J. Bolander. Three-dimensional lattice model for coupling of fracture and mass transport. In *Proceedings of Particles 2009*. European Community in computational methods in applied sciences (ECCOMAS), 2009.
- [9] P. Grassl and R. Rempling. A damage-plasticity interface approach to the meso-scale modelling of concrete subjected to cyclic compressive loading. *Engineering Fracture Mechanics*, 75(16):4804–4818, 2008.
- [10] H.J. Herrmann, A. Hansen, and S. Roux. Fracture of disordered, elastic lattices in two dimensions. *Physical Review B*, 39(1):637–648, 1989.
- [11] H. Nakamura, W. Srisoros, R. Yashiro, and M. Kunieda. Time-dependent structural analysis considering mass transfer to evaluate deterioration process of RC structures. *Journal of Advanced Concrete Technology*, 4:147–158, 2006.
- [12] H. R. Thomas R. W. Lewis, K. Morgan and K. N. Seetharamu. *The Finite Element Method in Heat Transfer Analysis*. John Wiley & Sons, 1996.
- [13] H. Sadouki and J. G. M. van Mier. Meso-level analysis of moisture flow in cement composites using a lattice-type approach. *Materials and Structures*, 30(204):579–587, December 1997.
- [14] E. Schlangen and J. G. M. van Mier. Simple lattice model for numerical simulation of fracture of concrete materials and structures. *Materials and Structures*, 25:534–542, 1992.
- [15] L. Wang, M. Soda, and T. Ueda. Simulation of chloride diffusivity for cracked concrete based on RBSM and truss network model. *Journal of Advanced Concrete Technology*, 6(1):143–155, 2008.

Appendix

MATLAB code

In the work presented, all simulations were undertaken using a code generated in MATLAB. The code consists of four parts. The first part is the node generator. To generate the nodes a number of parameters was needed to describe the domain such as, the domain dimensions and nodes density, which will determine number of nodes in the domain. Nodes are generated using a random number generator in MATLAB called (rand). X and Y coordinates of each node are generated separately. The nodes generated are restricted by the number of nodes P_1 3.1 and the minimum distance d_m between the nodes.

The second part of the code is discretisation of the domain. The discretisation is based on the nodes which were generated. To discretise the domain using the two methods Delaunay triangulation and Voronoi tessellation, Qhull was used. Qhull is a MATLAB package which can discretise the domain based on the nodes generated. The function used to generate the Delaunay triangulation is called (Delaunay). The function used to generate the Voronoi tessellation is called (Voronoi). The voronoi function was modified to obtain the elements topography in a different way than the origin function. The origin function sets the Voronoi polygon edges that tend to infinity as zero. The end nodes of these elements are first relocated to the boundary. They are then renumbered. For example, the topography matrix is as shown.

Appendix

$$\begin{bmatrix} 34 & 15 & 6 & 100 \\ 1 & 30 & 15 & 55 \\ 66 & 4 & 70 & 0 \\ 2 & 27 & 49 & 0 \end{bmatrix}$$

The first two numbers of the column present the Delaunay lattice elements nodes. The second two numbers present the Voronoi lattice element nodes that correspond to the Delaunay element. In the third column the number zero means that the coordinates of the Voronoi element node is (∞, ∞) . This point is therefore relocated to the boundary and given new appropriate coordinates.

The third part of the code is calculating the element stiffness matrix and assembling the global stiffness matrix to solve the temperature distribution of the domain. This was done with the help of a finite element toolbox called CALFEM [1]. The functions used were:

1. SPRINGLE, this function calculate each of the lattice element stiffness matrix.
2. ASSEM, this function was used to assemble the global stiffness matrix.
3. SOLVEQ, this function solves the system of equation in order to calculate the temperature distribution.
4. SPRINGLEM, this was a modified function of SPRINGLE, which calculates the heat capacitance matrix.

The fourth part of the code post-processing, where the nodal flux was calculated. The method was implemented in MATLAB by creating a new function called QFLUX, where the input was nodal temperatures, mesh topography, the lattice elements' cross-sectional areas, and the nodal coordinates. The output of the function is the nodal flux.

All the code, except of the Qhull and CALFEM functions, were written by the author.